

Removal of a Single α -Tubulin Gene Intron Suppresses Cell Cycle Arrest Phenotypes of Splicing Factor Mutations in *Saccharomyces cerevisiae*

C. Geoffrey Burns,^{1,2†} Ryoma Ohi,^{1,2‡} Sapna Mehta,^{1,2} Eileen T. O'Toole,³ Mark Winey,⁴ Tyson A. Clark,⁵ Charles W. Sugnet,⁵ Manuel Ares, Jr.,⁵ and Kathleen L. Gould^{1,2*}

Howard Hughes Medical Institute¹ and Department of Cell Biology,² Vanderbilt University School of Medicine, Nashville, Tennessee 37232; Boulder Laboratory for 3D Fine Structure³ and Department of Molecular, Cellular, and Developmental Biology,⁴ University of Colorado—Boulder, Boulder, Colorado 80309-0347; and Center for Molecular Biology of RNA, University of California, Santa Cruz, Santa Cruz, California 95064⁵

Received 18 September 2001/Accepted 1 November 2001

Genetic and biochemical studies of *Schizosaccharomyces pombe* and *Saccharomyces cerevisiae* have identified gene products that play essential functions in both pre-mRNA splicing and cell cycle control. Among these are the conserved, Myb-related CDC5 (also known as Cef1p in *S. cerevisiae*) proteins. The mechanism by which loss of CDC5/Cef1p function causes both splicing and cell cycle defects has been unclear. Here we provide evidence that cell cycle arrest in a new temperature-sensitive *CEF1* mutant, *cef1-13*, is an indirect consequence of defects in pre-mRNA splicing. Although *cef1-13* cells harbor global defects in pre-mRNA splicing discovered through intron microarray analysis, inefficient splicing of the α -tubulin-encoding *TUB1* mRNA was considered as a potential cause of the *cef1-13* cell cycle arrest because *cef1-13* cells arrest uniformly at G₂/M with many hallmarks of a defective microtubule cytoskeleton. Consistent with this possibility, *cef1-13* cells possess reduced levels of total *TUB1* mRNA and α -tubulin protein. Removing the intron from *TUB1* in *cef1-13* cells boosts *TUB1* mRNA and α -tubulin expression to near wild-type levels and restores microtubule stability in the *cef1-13* mutant. As a result, *cef1-13 tub1 Δ i* cells progress through mitosis and their cell cycle arrest phenotype is alleviated. Removing the *TUB1* intron from two other splicing mutants that arrest at G₂/M, *prp17 Δ* and *prp22-1* strains, permits nuclear division, but suppression of the cell cycle block is less efficient. Our data raise the possibility that although cell cycle arrest phenotypes in *prp* mutants can be explained by defects in pre-mRNA splicing, the transcript(s) whose inefficient splicing contributes to cell cycle arrest is likely to be *prp* mutant dependent.

Pre-mRNA splicing and cell cycle regulation have two distinct and apparently nonoverlapping functions for eukaryotic cells. In spite of this, a handful of genes in *Saccharomyces cerevisiae* and *Schizosaccharomyces pombe* have been identified in genetic screens for splicing factors (*prp* screens) and independently in screens for cell cycle regulators (*cdc* and related screens). These genes include *S. cerevisiae* *PRP3* (also known as *DBF5*), *PRP8* (also known as *DBF3*), *PRP17* (also known as *CDC40*), and *PRP22* and *S. pombe* *prp8*⁺ (also known as *cdc28*⁺) and *prp2*⁺ (also known as *mis11*⁺) (24, 26, 29, 44, 49, 56, 57). Furthermore, several *prp* mutants in *S. pombe* display morphologies consistent with defects in cell cycle progression (36, 54). Lastly, two proteins in *S. pombe*, Cdc5p and Dsk1p, both of which were identified genetically as potential cell cycle regulators, have since been implicated biochemically in pre-mRNA splicing (30, 50). In higher eukaryotes, splicing factors reorganize spatially throughout the cell cycle (19), and CDK2-

cyclin E phosphorylates the U2 snRNP protein, SAP155 (43). Collectively, these data raise the possibility that pre-mRNA splicing and cell cycle control are functionally linked in vivo, although the molecular mechanisms underlying this connection remain vague.

The conserved CDC5/Cef1p protein has been implicated in both pre-mRNA splicing and cell cycle control and exemplifies a potential link between these processes. The single temperature-sensitive allele of *cdc5*⁺, *cdc5-120*, arrests during the G₂ phase of the cell cycle prior to entry into mitosis (32, 34). *cdc5*⁺ encodes an essential protein with homology to the DNA binding domain of the transcription factor c-Myb (34). In its N terminus, Cdc5p contains two classic Myb repeats (R1 and R2) and a third nonclassic Myb-like repeat (MLR3) (33). To date, Cdc5p-related proteins have been isolated from every eukaryotic organism where they have been sought, including the budding yeast *S. cerevisiae*, where the homologous protein is termed Cef1p (7, 18, 22, 33, 48). The primary structure of CDC5/Cef1p has been conserved throughout evolution, with the Myb-related domains displaying the least divergence (33). We have concluded that this protein is also functionally conserved, since plant, fly, and human CDC5 cDNAs will rescue the temperature-sensitive lethality of *S. pombe* *cdc5-120* (22, 33). Furthermore, inactivation of CDC5/Cef1p in *S. cerevisiae* (33) and in mammalian cells (6) causes arrest or delay at G₂/M.

A major clue to the biochemical function of CDC5/Cef1p

* Corresponding author. Mailing address: Department of Cell Biology, Vanderbilt University School of Medicine, B2309 MCN, Nashville, TN 37232. Phone: (615) 343-9502. Fax: (615) 343-0723. E-mail: kathy.gould@mcmail.vanderbilt.edu.

† Present address: Cardiovascular Research Center, Massachusetts General Hospital, Charlestown, MA 02129.

‡ Present address: Department of Cell Biology, Harvard Medical School, Boston, MA 02115.

TABLE 1. Yeast strains used in this study

Strain	Relevant genotype	Source
YPH98	<i>MATa ade2-101 leu2-Δ1 lys2-801 trp1-Δ1 ura3-52</i>	P. A. Weil
YPH252	<i>MATα ade2-101 his3-Δ200 leu2-Δ1 lys2-801 trp1-Δ1 ura3-52</i>	P. A. Weil
KGY1522	<i>MATa cef1-13 ade2-101 leu2-Δ1 lys2-801 trp1-Δ1 ura3-52</i>	This study
KGY1760	<i>MATa cdc28-1N</i>	S. Reed
KGY1825	<i>MATa prp3-1 ade1 ade2 ura1 tyr1 his7 lys2 gal1</i>	B. Rymond
KGY1229	<i>MATa prp18-1 ade2-101 his3Δ200 tyr1 ura3-52</i>	J. Patton
KGY2914	<i>MATa tub1Δi ade2-101 leu2-Δ1 lys2-801 trp1-Δ1 ura3-52</i>	This study
KGY2915	<i>MATa cef1-13 tub1Δi ade2-101 leu2-Δ1 lys2-801 trp1-Δ1 ura3-52</i>	This study
KGY2818	<i>MATa prp17/cdc40Δ his3Δ1 leu1Δ0 met15Δ ura3Δ0</i>	M. Ares
KGY2917	<i>MATa prp17/cdc40Δ tub1Δi his3Δ1 leu1Δ0 met15Δ0 ura3Δ0</i>	This study
KGY2847	<i>MATa prp22-1 ade2 his3 ura3</i>	This study
KGY2918	<i>MATa prp22-1 tub1Δi ade2 his3 ura3</i>	This study
CKY569	<i>MATa rse1-1 SAR1-Δi ura3-52 leu2-3,112</i>	Chris Kaiser
KGY3179	<i>MATa rse1-1 SAR1-Δi ura3-52 leu2-3,112 cef1-13</i>	This study

proteins came when human CDC5 (hCDC5) (also called CDC5L) was isolated in a biochemical purification of the mammalian spliceosome (31). Several lines of evidence have since established that these proteins play an essential role in pre-mRNA splicing. CDC5 colocalizes with pre-mRNA splicing factors in the nuclei of mammalian cells (11), *S. pombe* Cdc5p and hCDC5 associate with core components of the splicing machinery (11, 30), *S. cerevisiae* Cef1p and hCDC5 interact with the spliceosome in vitro (1, 11, 53), and genetic depletion of *S. cerevisiae* Cef1p or *S. pombe* Cdc5p causes accumulation of unspliced mRNAs in vivo (11, 30, 53). Lastly, Cef1p and hCDC5 play direct roles in pre-mRNA splicing, because inactivation of Cef1p by antibody interference or immunodepletion of hCDC5 inhibits splicing in vitro (1, 53).

In vivo, all detectable fission yeast Cdc5p is associated with a large (~40S) multiprotein complex. This particle has been purified by immunoaffinity chromatography, and the identities of 10 Cwf (complexed with cdc5p) proteins have been reported (30). Significantly, most of the Cwf proteins have been directly or indirectly (through homologs in other organisms) implicated in the process of pre-mRNA splicing. *S. cerevisiae* Cef1p also resides in a protein complex identified through immunoaffinity purification of the splicing factor Prp19p (51, 53). It is likely that the fission yeast Cdc5p- and budding yeast Prp19p-associated protein complexes represent equivalent or related complexes. Lastly, hCDC5 copurifies with many proteins whose identities as known splicing factors were recently reported (1).

Although these data strongly implicate CDC5/Cef1p proteins biochemically and genetically in pre-mRNA splicing, it was unclear how they would also be required for cell cycle progression. Interestingly, phenotypic characterization of *S. cerevisiae* *cef1*-null cells revealed that, in addition to harboring splicing and cell cycle defects, these cells also failed to assemble mitotic spindles (33). This observation suggested the possibility that defective microtubules might be mediating cell cycle arrest in these cells.

To investigate the function of CDC5/Cef1p proteins in cell cycle control and pre-mRNA splicing, we analyzed a novel temperature-sensitive allele of *CEF1*, *cef1-13*. Like *cef1*-null cells, *cef1-13* cells displayed defects in both processes. Many of the *cef1-13* phenotypes, including cell cycle arrest at G₂/M, could be suppressed by removing the intron from one of the

genes encoding α -tubulin (*TUB1*). These data indicate that defective pre-mRNA splicing is the primary defect in *cef1-13* cells. Removing the *TUB1* intron from two other splicing mutants that arrest in G₂/M, *prp17Δ* and *prp22-1* strains, only partially suppressed their cell cycle phenotypes. Our data indicate that inefficient splicing of *TUB1* is a significant contributor to the G₂/M arrest phenotype observed in these splicing mutants. Moreover, our data are consistent with the idea that cell cycle phenotypes of yeast *prp* mutants can likely be explained as indirect consequences of pre-mRNA splicing defects.

MATERIALS AND METHODS

Strains, growth media, and genetic methods. All *S. cerevisiae* strains used in this study are listed in Table 1. Strains produced in our laboratory are derivatives of S288C. *prp3-1* (57), *prp17* (also known as *CDC40Δ*; Research Genetics, Huntsville, Ala.), *prp18-1* (57), *prp22-1* (57), *cdc28-1N* (38), and *sar1Δi* (12) strains were obtained from other sources (Table 1). Strains obtained from other laboratories, with the exception of *prp3-1*, *prp18-1*, *cdc28-1N*, and *sar1Δi* strains, were backcrossed a minimum of three times against YPH98 or YPH252 prior to use. Strains were grown in yeast extract-peptone (YEP) medium supplemented with 2% glucose (YPD) or synthetic minimal medium with the appropriate nutritional supplements. Genetic methods were as described (20). Transformation of *S. cerevisiae* was performed by the lithium acetate method (25). Permissive temperature for all strains was 25°C, and restrictive temperature was between 35.5 and 37°C.

Benomyl (Sigma, St. Louis, Mo.) was diluted into YPD agar at the concentrations indicated from a stock solution of 10 mg/ml in dimethyl sulfoxide.

Construction of *cef1-13*. The *cef1-13* mutant allele (33) was subcloned by ligating the *Bam*HI/*Hind*III fragment of pRO148 (pRS415 which harbors the *cef1-13* allele [33]) into *Bam*HI/*Hind*III cleaved pRS406Δ*Cla*I to generate pRO173. pRS406Δ*Cla*I was constructed by linearizing pRS406 with *Cla*I, treating the linearized vector with Klenow fragment, and ligating the vector on itself. pRO173 was linearized with *Cla*I and transformed into YPH98 cells with selection applied for Ura prototrophy, and colonies were screened by Southern analysis to identify those transformants that had integrated the plasmid at the *CEF1* locus. One such transformant was plated onto 5-fluoroorotic acid (5-FOA) medium to select for excision events, and these colonies were screened for temperature sensitivity. KGY1522 is a single temperature-sensitive clone that arose from these manipulations.

Oligonucleotide arrays. We use the terms "probe" and "target" where the probe is the known sequence (in this case, the oligonucleotide on the array) and the target is the unknown sequence (in this case, the fluor-labeled cDNA), regardless of which sequence carries the label or which sequence is immobilized. A set of 40-mer oligonucleotide probes carrying 5' amino linked modifications was synthesized by Weboligos, Inc. Sequences were chosen to be complementary to cDNAs produced by reverse transcription of yeast intron-containing gene transcripts (13; http://www.cse.ucsc.edu/research/compbio/yeast_introns.html). The splice junction oligonucleotide probes span the splice junctions with 20

residues from each exon. The intron and second-exon probes were selected using a set of criteria to match predicted melting temperatures and to contain little internal structure, high information content, and low similarity to secondary sites in the genome. Probes were also synthesized to measure levels of eight intronless yeast mRNAs whose levels do not vary in numerous microarray experiments performed by the Brown laboratory (<http://cngm.stanford.edu/~pbrown>) for normalization. In experiments with more than 30 different mutations in splicing factor genes, we observe increased levels of intron-containing transcripts and decreased levels of splice junction-containing transcripts, with variable (gene-specific) decreases in second-exon transcripts that indicate general splicing defects such as that exhibited by *cef1-13*. The details of that work (T. A. Clark, C. W. Sugnet, and M. Ares, Jr., unpublished data) will be presented elsewhere.

Removal of the *TUB1* intron from wild-type, *cef1-13*, *prp17Δ*, and *prp22-1* cells. The *TUB1* gene, including 350 to 550 bp 5' and 3' of the open reading frame, was PCR amplified as two overlapping fragments from wild-type genomic DNA and cloned into pBluescript SK (Stratagene, La Jolla, Calif.). The primer pairs TUB1.1 (5'-AACTGCAGCCATTATAACTGACTGTTTCAGATCCTGC-3')-TUB1.1int (5'-GCAAAGCTTGGTCTTGGGATATCC-3') and TUB1.2 (5'-A ACTGCAGTACCGGTTCTGTTTACCTTCTAATG-3')-TUB1.2int (5'-G GAATTTGCCGTATACCCTGCTCC-3') were used to generate the 5' and 3' fragments respectively of the *TUB1* insert. Both fragments were digested with *Pst*I/*Hind*III and placed into a three-part ligation with *Pst*I-digested pBluescript SK to create pSK*TUB1*. The single intron within *TUB1* that resides in codon 9 was precisely deleted using the Chameleon double-stranded site-direct mutagenesis kit (Stratagene) with TUB1.3 (5'-CCCAACAGGCATTACCAATCTGAC AACCAGCTTGACCAGACATTAATAGATATCACTTCTCTCATTGTTTGT TTGC-3') and TUB1.4 (5'-GCGGCCGCTCTAGAACTAGTGGAAACCCCG GGTGCAGGAATTCGATATCAAGC-3') as the mutagenic and selection primers, respectively, to create pSK*tub1Δ*. The mutagenic primer engineered an *Eco*RV site spanning codons 4, 5, and 6 of *TUB1* that conserved the Tub1p amino acid sequence. The insert in pSK*tub1Δ* was completely sequenced to verify its accuracy.

Transplacement (42) was used to replace the endogenous *TUB1* allele with the intronless *tub1Δ* allele in YPH98, YPH1522, KGY2849, and KGY2818. The *tub1Δ* allele was subcloned by ligating the *Sal*I/*Xma*I fragment of pSK*tub1Δ* into the *Sal*I/*Xma*I-cleaved integrating vector pRS406 to generate pRS406*tub1Δ*. The *Sal*I/*Xma*I fragment from pRS406*tub1Δ*, which contains all of the DNA sequence downstream of codon 94, was excised from pRS406*tub1Δ* to create the integrating construct termed "pRS406*tub1Δ* *Bcl*I/*Bam*HI delete." pRS406*tub1Δ* *Bcl*I/*Bam*HI delete was used as the integrating construct instead of pRS406*tub1Δ* to decrease the probability that the wild-type locus would be re-created upon excision of the integrated plasmid. pRS406*tub1Δ* *Bcl*I/*Bam*HI delete was cut at the *Bsa*BI site, which is downstream of the exon 1-exon 2 junction, and transformed into the strains listed above. Transformants in which pRS406*tub1Δ* *Bcl*I/*Bam*HI delete had been integrated correctly at the *TUB1* locus were identified by Ura auxotrophy and Southern analysis. One such transformant for each parent strain was plated onto 5-fluoroorotic acid medium, and colonies in which *TUB1* had been replaced with *tub1Δ* were identified by Southern blot analysis. For Southern blot analysis, the genomic DNA was digested with *Eco*RV and probed with the *Xma*I/*Sal*I fragment from pSK*tub1Δ*.

Construction of *cef1-13 sar1Δ*. A *cef1-13 sar1Δ* strain was identified in a tetrad derived from a cross between KGY1522 and KGY2860 in which all four colonies were temperature sensitive. Genomic DNA from each colony in the tetrad was subjected to PCR analysis. The *SAR1* and *sar1Δ* alleles segregated 2:2 in this cross and were identified by the generation of a 463- or 324-bp band, respectively, in PCRs using the SAR15' (5'-GGCTGGTTGGGATATTTTTT G-3') and SAR13' (5'-GCTTCATCAAAATCTTCAGGG-3') primers. The *CEF1* and *cef1-13* alleles also segregated 2:2 and were identified by whether the PCR fragment generated with the primers R1R25' (5'-CGCGGATCCGCATG CCCCCGTACCAATATACGTGAAAGCCGG-3') and MLR33' (5'-CCTCT GCAGTCTGCTTGCTTTAGCTACCGCTCTTTTGTAGTTCAGC-3') were resistant or sensitive, respectively, to digestion with *Pvu*I.

Cell synchronization. Exponentially growing cells were arrested in G_1 by incubation in the presence of α -factor (10 μ g/ml; Sigma) for 180 min at 25°C. To release cells from α -factor, cells were washed with 3 to 5 volumes of YPD and resuspended in fresh YPD prewarmed to between 35.5 and 37°C. For synchronization of cells with plasmids, the cells were grown overnight in selective medium and then synchronized and released in YPD medium.

Cytological methods and flow cytometry. To visualize nuclei, cells were fixed with 70% ethanol overnight at 4°C, washed twice with phosphate-buffered saline, and resuspended in 1 μ g of DAPI (4',6'-diamidino-2-phenylindole) per ml. Cells were prepared for indirect immunofluorescence as described (37). α -Tubulin was detected using the monoclonal antibody TAT-1 (60) at a dilution of 1:50 fol-

lowed by an Alexa 594-conjugated goat anti-mouse secondary antibody (Molecular Probes, Eugene, Oreg.).

Cells for flow cytometric analysis were fixed in ice-cold 70% ethanol, sonicated for 15 s in 1 ml of 50 mM sodium citrate (pH 7.0) containing 0.25 mg of RNase A per ml, and incubated overnight at 37°C. Cells were then stained with 1 μ M Sytox Green (Molecular Probes) in 1 ml of 50 mM sodium citrate (pH 7.0) for at least 1 h at 4°C in the dark. The DNA content was measured on a Becton Dickinson FACSCalibur as described (15).

Electron microscopy. Asynchronous, exponentially growing KGY1522 cells were shifted to 35.5°C for 3 h, fixed by high-pressure freezing, and processed for electron microscopy as described (17).

Immunoblot analysis and histone H1 kinase assays. For immunoblot analyses, protein extracts were prepared from frozen cell pellets by glass bead disruption of cell walls. Lysed cells were heated to 95°C in SDS lysis buffer (10 mM NaPO₄ [pH 7.4], 1.0% sodium dodecyl sulfate [SDS], 1 mM dithiothreitol, 1 mM EDTA, 50 mM NaF, 100 μ M Na₂VO₄, leupeptin [4 μ g/ml]) for 1 to 3 min and extracted with NP-40 buffer (6 mM Na₂HPO₄, 4 mM NaH₂PO₄, 1.0% NP-40, 150 mM NaCl, 2 mM EDTA, 50 mM NaF, 100 μ M Na₂VO₄, leupeptin [4 μ g/ml]) supplemented with protease inhibitors (Complete; Boehringer Mannheim, Mannheim, Germany). Lysates were clarified to remove cell debris by microcentrifugation. Bicinchoninic acid assays (Pierce, Rockford, Ill.) were performed, and the total amount of protein in each sample was normalized based on these measurements. SDS sample buffer (5 \times) was added, and the samples were heated to 95°C prior to electrophoresis.

Protein extracts were fractionated on Novex NuPAGE 4 to 12% bis-Tris gels using NuPAGE MOPS SDS running buffer (Invitrogen, Carlsbad, Calif.) and subsequently transferred to Immobilon P membranes (Millipore Corp., Bedford, Mass.). Proteins were detected using an enhanced chemiluminescence detection system (ECL+Plus; Amersham Pharmacia Biotech, Piscataway, N.J.) and visualized by either film exposure or fluorescence scanning (Storm Phosphorimager; Molecular Dynamics Inc., Sunnyvale, Calif.). α -Tubulin was detected using TAT-1 monoclonal antibody at a dilution of 1:1,000. TATA binding protein (35) and Clb2p (28) were detected using affinity-purified polyclonal antisera at dilutions of 1:10,000 and 1:1,000 respectively. PSTAIRE antibodies (Sigma) were used at a dilution of 1:5,000. Goat anti-rabbit and anti-mouse secondary antibodies (Jackson Immunoresearch Laboratories, Inc.) were used at a dilution of 1:50,000.

Histone H1 kinase assays were performed as described previously (28) using affinity-purified rabbit anti-Clb2p polyclonal antibodies.

Other techniques. For determination of cell numbers, samples were prepared and analyzed on a Multisizer II device (Beckman Coulter Inc., Fullerton, Calif.) as described (33). For determination of cell viability, cell numbers were assessed at each time point and 300 cells were plated in triplicate onto YPD agar at 25°C. The number of colonies per plate was counted 48 h later. Preparation of RNA and Northern blotting were performed as described (11). The *TUB1*, *TUB2*, and *TUB3* open reading frames were obtained from Research Genetics.

RESULTS

***cef1-13* cells arrest in G_2/M with unstable microtubules.** *S. cerevisiae* cells lacking endogenous *CEF1* and harboring a *CEN* plasmid-borne mutant allele of *CEF1*, *cef1-13*, are temperature sensitive for growth (33). Cef1p contains two amino acid substitutions, Trp52 to Gly and Trp84 to Gly, which are located at the third hydrophobic residue in R1 and the second hydrophobic residue in R2, respectively (33). To construct a stable version of the *cef1-13* allele, the above mutations were introduced into the chromosomal copy of *CEF1* in a wild-type haploid strain (see Materials and Methods). Although *cef1-13* cells were unable to grow at the restrictive temperature, a diploid strain carrying one copy of the *cef1-13* allele was viable at the same temperature, indicating that the *cef1-13* allele is recessive.

To characterize the cell cycle arrest phenotype of *cef1-13* cells, we synchronized wild-type and *cef1-13* cells in G_1 with α -factor and then released the cells at the restrictive temperature. The released cells were monitored for cell number and cell cycle progression as reflected by DNA content. In the time

following release, the cell number for the wild-type culture increased exponentially, whereas that for the *cef1-13* culture remained unchanged (Fig. 1A). Analysis of DNA content revealed that both wild-type and *cef1-13* cells completed a full round of DNA replication (Fig. 1B). Subsequently, wild-type cells progressed normally into the next cell cycle, whereas *cef1-13* cells arrested homogeneously in G₂/M (Fig. 1B). At 4 h following release, the cell number (Fig. 1A) and DNA profile (data not shown) for the *cef1-13* cells were indistinguishable from those at 3 h, indicating that the cells had arrested by 3 h. *cef1-13* cells contained high Clb2p levels and Clb2p-associated H1 kinase activity at 3 h following release, demonstrating that *cef1-13* cells arrested with activated mitotic CDKs (see below). Evaluation of bud and nuclear morphologies revealed that the majority of *cef1-13* cells arrested with large buds and contained a single nucleus in the mother cell (Table 2). Whereas wild-type cells displayed 100% viability at this time, only 45% of *cef1-13* cells were viable. These data suggest that *cef1-13* cells arrest in the first cell cycle during G₂/M prior to anaphase. Like synchronized cultures, asynchronous *cef1-13* cultures arrested with large buds in G₂/M within 3 h following shift to the restrictive temperature (data not shown).

A notable feature of the *cef1-13* arrest phenotype was the presence of large budded cells that had failed to position their nuclei at the mother-bud junction in preparation for mitosis. These defects were seen in approximately 30% of the entire cell population and in 40% of the large-budded cells (Table 2) and were similar to those seen in *cef1*-null cells (33). Because large buds and nuclear positioning defects are hallmarks of cells with defective microtubules (41), we evaluated the state of microtubules in arrested *cef1-13* cells by indirect immunofluorescence following formaldehyde fixation with a monoclonal antibody raised against α -tubulin (60). Approximately 75% of *cef1-13* cells lacked visible nuclear and cytoplasmic microtubules, leaving only a small spot of staining near the nucleus (Fig. 1C), most likely at the spindle pole body (SPB). In roughly half of these cells, very short microtubules emanated from the single spot of staining (Fig. 1C). The remaining 25% of cells contained either a short intranuclear spindle with very short cytoplasmic microtubules or an extended mitotic spindle contained entirely within the mother cell (Fig. 1C). The microtubule defects observed in *cef1-13* cells were never seen in wild-type cells prepared in parallel (Fig. 1C). *cef1-13* cells fixed with methanol also lacked visible microtubules (data not shown). These data suggest that *cef1-13* cells are defective in assembling or maintaining stable microtubules.

That a single focus of α -tubulin staining was observed by immunofluorescence suggested that *cef1-13* cells contained either one unduplicated SPB or duplicated SPBs that failed to separate. To clarify this issue, we analyzed arrested *cef1-13* cells by electron microscopy. Cells were prepared using high-pressure freezing and freeze substitution (HPF-FS) fixation rather than chemical fixation because yeast cells prepared with HPF-FS display less distortion in microtubule structures (17). In seven of seven cells, SPBs had duplicated, were morphologically normal, and had separated to various degrees (Fig. 1D). In all cells observed, intact microtubules emanated from both the nuclear (Fig. 1D) and cytoplasmic (data not shown) faces of SPBs. Surprisingly, five of seven cells contained fully assembled spindles (Fig. 1D, data not shown). However, these spin-

dles were abnormal in that they appeared to exert a force on the nuclear envelope because it was invaginated where the SPBs were inserted. This phenotype is never observed in wild-type cells prepared by HPF-FS (17). We interpret this to mean that spindles assembled in *cef1-13* cells are prone to collapse because they are built with unstable microtubules. It is likely that the chemical fixation of *cef1-13* cells used during processing for indirect immunofluorescence induced a complete collapse of the spindle. Collectively, these data are consistent with the idea that microtubules in *cef1-13* cells are inherently unstable.

Because mutants with defective microtubules often display hypersensitivity to the microtubule depolymerizing drug benomyl (41), we determined if *cef1-13* cells were benomyl sensitive. Whereas wild-type cells formed colonies on benomyl (15 μ g/ml), the *cef1-13* mutant was unable to form colonies under the same conditions (Fig. 1E), indicating that the *cef1-13* mutant is hypersensitive to benomyl.

***cef1-13* cell are defective in pre-mRNA splicing.** Because CDC5/Cef1p proteins have been implicated directly in pre-mRNA splicing (1, 11, 53), we analyzed *cef1-13* cells to determine if pre-mRNA splicing defects were present and how widespread the defects were. We utilized splicing-sensitive oligonucleotide microarrays (Clark et al., submitted for publication) for this purpose and compared the levels of spliced and unspliced RNAs from the complete set of intron-containing genes in wild-type and *cef1-13* cells. Total RNA was prepared from wild-type and *cef1-13* cells soon after they had entered G₂ following release from α -factor (60 and 90 min following release for wild-type and *cef1-13* cells, respectively; see Fig. 1B) and used these as templates for the synthesis of fluorescent cDNA target sequences by reverse transcription. The target cDNAs were competitively hybridized to oligonucleotide microarrays containing probes for the intron, the splice junction, and the second exon sequence for yeast intron-containing genes (Clark et al., submitted). Out of 204 intron probes, 191 (94%) had signals indicating that their targets were more abundant in *cef1-13* cells than in wild-type cells, indicating accumulation of unspliced RNA in *cef1-13* cells (Fig. 2). Out of 419 targets detected by the splice junction and second exon probes, 400 (95%) were less abundant in *cef1-13* cells, indicating that *cef1-13* cells are generally depleted of spliced mRNAs. Transcripts that were most affected by the *cef1-13* mutation are listed in Table 3. Cluster analysis of the *cef1-13* profile indicated that the defects seen in *cef1-13* are similar to those observed upon inactivation of the temperature-sensitive splicing mutant *prp4-1* and are more severe than those caused by deletion of most nonessential splicing factors (data not shown).

In analyzing these data with respect to the cell cycle, we searched the yeast intron database (13, 46) for intron-containing genes known to have a role in microtubule function and cell cycle progression. Three such genes were considered: *TUB1* and *TUB3*, the two genes encoding α -tubulin (39, 40), and *GIM5*, a gene required for correct folding of tubulin subunits (16). Although all the spliced forms of the mRNAs from these genes were decreased in the *cef1-13* mutant (Table 3), and mutations in each are reported to cause sensitivity to benomyl (16, 40, 41, 47), only *TUB1* is an essential gene (40), and therefore, it became the focus of our attention.

***cef1-13* cell have less total *TUB1* mRNA and α -tubulin protein at the restrictive temperature.** To confirm that *TUB1*

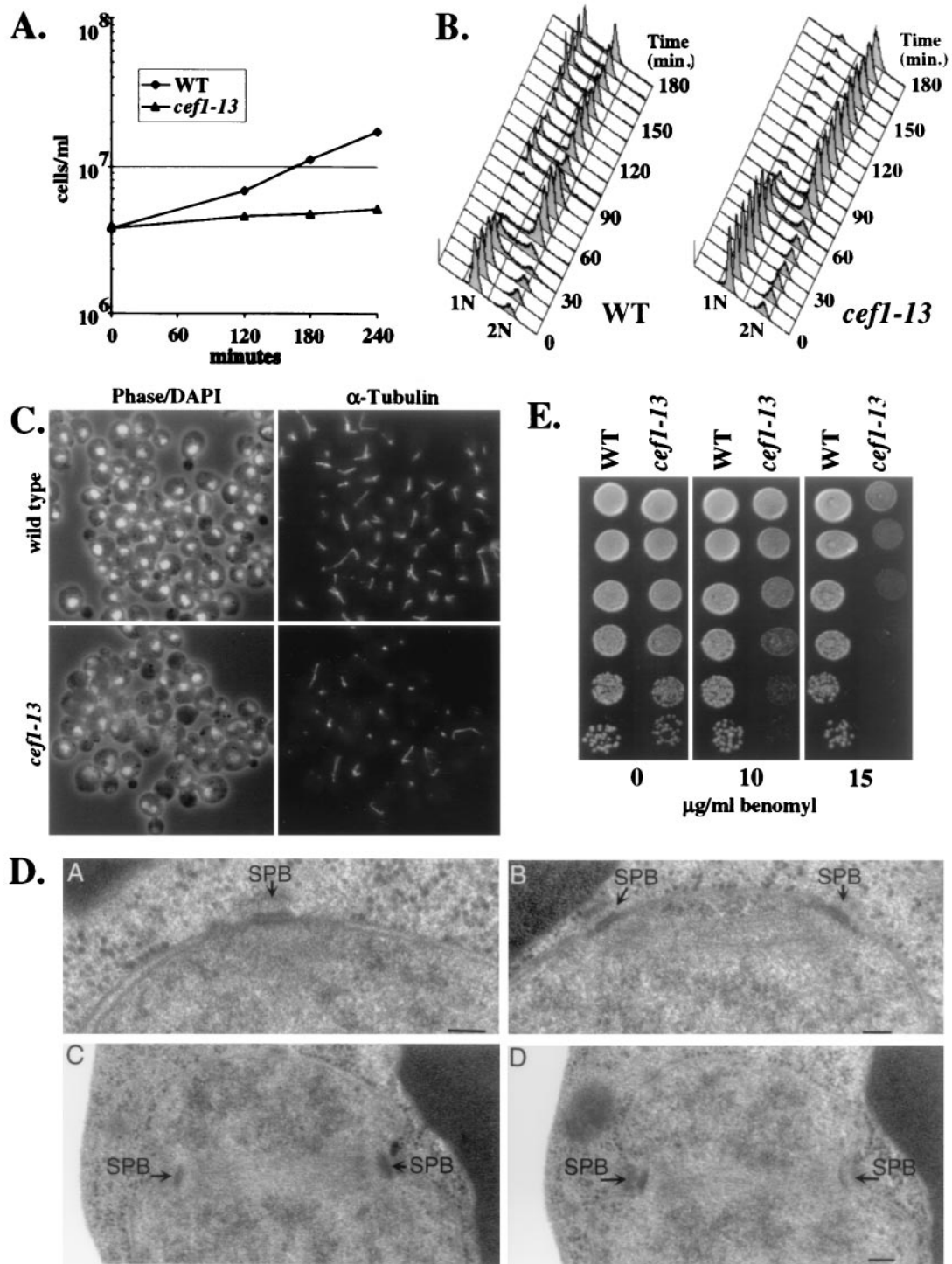








FIG. 1. The *cef1-13* mutant arrests at G_2/M with unstable microtubules. Wild-type (WT) and *cef1-13* cells were synchronized in G_1 and released to the restrictive temperature. Cell number (A) and fluorescence-activated cell sorter analysis (B) for each strain following release are shown. (C) Staining of microtubules in G_2/M -arrested *cef1-13* cells. Asynchronous cultures of WT or *cef1-13* cells were shifted to the restrictive temperature for 3 h and stained for microtubules using an anti- α -tubulin antibody (TAT-1) (60) followed by an Alexa 594-conjugated secondary antibody. DNA was visualized using DAPI. (D) Electron micrograph analysis of the *cef1-13* mutant. An asynchronous culture of *cef1-13* cells was shifted to the restrictive temperature for 3 h and processed for electron micrograph analysis by HPS-FS. (Subpanel A) A 50-nm-thin section of an SPB which exhibits a wild-type trilaminar organization. (Subpanel B) Thin section through a short bipolar spindle with both SPBs in the plane of the section. (Subpanels C and D) Two serial semithick (100-nm) sections showing a short bipolar spindle with accompanying involutions of the nuclear membrane. (E) *cef1-13* is benomyl sensitive. WT and *cef1-13* cells were serially diluted fivefold from a culture at an optical density at 600 nm of 1.0 and spotted onto YPD plates or YPD plates containing the indicated concentrations of benomyl.

TABLE 2. Quantitation of cell and nuclear morphologies 180 min following release from α -factor

Cell	% of total cells displaying indicated morphology ^a							n ^b
							Other	
Wild type	46	25	9	1	7	11	2	400
<i>tub1</i> Δ i	46	24	10	0	5	13	2	400
<i>cef1-13</i>	12	5	43	29	3	5	4	404
<i>cef1-13 tub1</i> Δ i	41	17	6	2	5	26	3	410

^a Each morphologic class is shown schematically. Large-budded cells were scored if the bud was equal to or greater than half of the size of the mother. The percentages do not always add up to 100% due to rounding.

^b n, total number of cells counted.

expression was reduced in *cef1-13* cells, we quantified the amount of total *TUB1* mRNA by Northern analysis in wild-type and *cef1-13* cells shifted to the restrictive temperature. *cef1-13* cells contained roughly half the amount of *TUB1* message that wild-type cells had (Fig. 3A to C). In shifted asynchronous cells, *TUB1* message declined to approximately 20% of the level seen in wild-type cells (Fig. 3A). Two other splicing mutants, *prp3-1* and *prp18-1*, that are defective in the first and second steps of pre-mRNA splicing, respectively, also dis-

played decreased levels of *TUB1* at the restrictive temperature (Fig. 3A). However, a cell cycle mutant that arrests in G₂/M, *cdc28-1N* (38), did not display a significant decrease in total *TUB1* (Fig. 3A), demonstrating that loss of *TUB1* mRNA is not a consequence of cell cycle arrest in G₂/M. Another intron-containing transcript, *TUB3*, was decreased by approximately 50% in synchronous (Fig. 2C and 3B) and in asynchronous (data not shown) *cef1-13* cultures shifted to the restrictive temperature. However, neither of two intronless transcripts, *TDH2* (the loading control for all of the Northern blots) and *TUB2*, was decreased significantly in synchronous *cef1-13* cultures shifted to the restrictive temperature (Fig. 3B and C). These data validate the microarray analysis and indicate that *TUB1* mRNA levels are reduced in *cef1-13* cells. Because the *TUB1* intron is very small, it is technically difficult to detect its pre-mRNAs by Northern blot analysis (data not shown). However, using multimerized intron sequences as probes, we were able to conclude that the *TUB1* pre-mRNA did not accumulate to the same extent in *cef1-13* cells as in the *prp3-1* mutant (data not shown). However, it has recently been demonstrated that pre-mRNAs do not accumulate significantly in many pre-mRNA splicing mutants because they are degraded by the exosome complex (8).

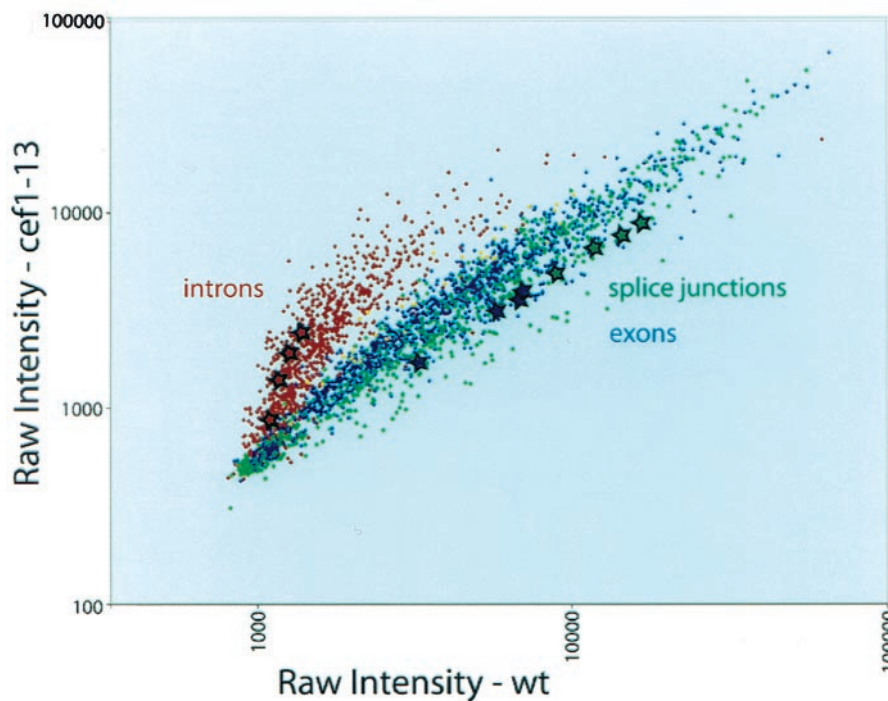


FIG. 2. Scatter plot of *cef1-13* versus wild-type (wt) splicing microarray data. RNA from the *cef1-13* mutant was used as a template for reverse transcription in the presence of Cy5-dUTP, and RNA from wt cells was used as a template in the presence of Cy3-dUTP. The labeled target cDNAs were mixed and hybridized to the oligonucleotide probes on a printed microarray (see Materials and Methods). After washing, the array was scanned and the image analyzed to extract the data. Each point in the plot represents raw intensity data from a single probe spot, with the Cy3 (wt) signal on the abscissa and the Cy5 (mutant) signal on the ordinate. Each probe is present four times on the array. Intron probes (specific to unspliced RNA) are labeled in red, splice junction probes (specific to spliced RNA) are labeled in green, exon probes (representing total gene specific RNA) are labeled in blue, and non-intron-containing gene probes used for normalization are labeled in yellow. The four spots representing each of the *TUB1*-specific oligonucleotides are labeled with stars. Two factors influence the absolute intensity measurements, so it is important to keep in mind that the Cy5/Cy3 ratio is the key indicator of the difference between mutant and wt. First, different oligonucleotides have distinct hybridization properties, making direct comparison of absolute intensities uninformative. Second, since the identical probe is spotted in different positions on the array, their absolute intensities vary due to local hybridization differences. Note that each set of four identical probes falls in a line, indicating a consistent Cy5/Cy3 ratio measurement.

TABLE 3. Transcripts whose splicing is most defective in *cef1-13* cells^a

Transcript with change in splicing	Transcript with change in splicing
Increased in <i>cef1-13</i>	
Intron	
<i>QCR10</i>	<i>RPS10A</i>
<i>COF1</i>	<i>RPL16B</i>
<i>ACT1</i>	<i>RPL21B</i>
<i>MATA1-Int1</i>	<i>RPS8A</i>
<i>YNL050c</i>	<i>RPS23A</i>
<i>RUB1</i>	<i>RPL6A</i>
<i>SRC1-Int1</i>	<i>RPL40A</i>
<i>SRC1-Int2</i>	<i>SAR1</i>
<i>RPL39</i>	<i>YKL002w</i>
<i>RPL33A</i>	<i>UBC13</i>
<i>RPL34A</i>	<i>UBC4</i>
<i>RPL27B</i>	<i>RPL23A</i>
<i>ARP9</i>	<i>NCB2</i>
<i>YBL059w</i>	<i>CNB1</i>
<i>ARP2</i>	<i>YML056c</i>
<i>MMS2</i>	<i>RPL26B</i>
<i>RPL17A</i>	<i>RPL32</i>
<i>YIP3</i>	<i>SEC14</i>
<i>MATA1-Int2</i>	<i>PMI40</i>
<i>RPS27B</i>	<i>RPL40B</i>
<i>RPS23B</i>	
<i>RPS19A</i>	Decreased in <i>cef1-13</i>
<i>RPL7B-Int2</i>	Intron
<i>RPL25</i>	<i>RPS22B-Int2</i>
<i>ERD2</i>	
<i>MUD1</i>	Splice junction
<i>RPL33B</i>	<i>SEC14</i>
<i>RPL21A</i>	<i>MMS2</i>
<i>OST5</i>	<i>GIM5</i>
<i>YDR367w</i>	<i>RPL23A</i>
<i>RPL37A</i>	<i>YGL232w</i>
<i>YPR063c</i>	<i>YKL158w</i>
<i>MAF1</i>	<i>COF1</i>
<i>RPL34B</i>	<i>QCR10</i>
<i>RPS30A</i>	<i>RPS22B-SJ1</i>
<i>YDL012c</i>	<i>SEC27</i>
<i>DYN2-Int2</i>	<i>YBR230c</i>
<i>SNC1</i>	<i>PFY1</i>
<i>RPL27A</i>	<i>COX4</i>
<i>RIM1</i>	<i>YLR128w</i>
<i>SNR17b</i>	<i>RPL16A</i>
<i>YML067c</i>	<i>MATA1-SJ2</i>
<i>NYV1</i>	<i>STO1</i>
<i>RPL23B</i>	<i>TUB3</i>
<i>RPO26</i>	<i>RPL30</i>
<i>RPS10B</i>	<i>RPS22B-SJ2</i>
<i>QCR9</i>	<i>RPS26B</i>
<i>YGL232w</i>	<i>YLR211c</i>
<i>RPS21B</i>	<i>TUB1</i>
<i>IST1</i>	<i>RPS25B</i>
<i>LSM2</i>	<i>HNT2</i>
<i>RPS30B</i>	<i>NCE101</i>
<i>YIP2</i>	<i>RPL22B</i>
<i>RPS6A</i>	<i>ANC1</i>
<i>RPL29</i>	<i>NMD2</i>
<i>YLR128w</i>	<i>RPL27B</i>
<i>RPL37B</i>	<i>RPL22A</i>
<i>RPS7A</i>	<i>YKL002w</i>
<i>RPS26A</i>	<i>UBC12</i>
<i>RPS16A</i>	<i>RPL13A</i>
<i>TUB1</i>	<i>RPL35B</i>
<i>RPL18A</i>	<i>RPL18B</i>
<i>RPL16A</i>	<i>YHR097c</i>
	<i>RPL27A</i>
	<i>OST5</i>

^a Total RNA from wild-type and *cef1-13* cells that were cell cycle staged at G₂/M was competitively hybridized to oligonucleotide microarrays containing probes for the intron and splice junction for yeast intron-containing genes. The transcripts that were increased or decreased twofold or more in *cef1-13* cells for each class of probe are listed in decreasing order of fold difference between the mRNA samples. *TUB1*, *TUB3*, and *GIM5* are shown in boldface type because of their importance for microtubule biogenesis. Raw numbers for the first and last transcript on each list as well as the highlighted transcripts are given here. Fold differences (expressed as *cef1-13* relative to wild type) are given in parentheses. The medians for each class are also given. Intron probes: *QCR10* (4.87), *TUB1* (2.22), *RPL40B* (2.01); median, 1.84. Splice-junction probes: *SEC14* (-4.27), *GIM5* (-3.96), *TUB3* (-2.36), *TUB1* (-2.30), *OST5* (-2.00); median, -1.53.

To determine whether the decrease in *TUB1* mRNA translated to a decrease in protein levels, α -tubulin protein levels in wild-type and *cef1-13* cells were determined by immunoblotting 3 h following shift to the restrictive temperature. Given that the *TUB1* mRNA was decreased by only 50% on average, we did not expect to detect a large decrease in α -tubulin protein levels. For this reason, we examined α -tubulin protein levels multiple times in two independent experiments and present the results of these immunoblotting experiments graphically. Following quantitation, we determined that α -tubulin protein levels in *cef1-13* cells were 72% of the level found in wild-type cells (Fig. 3D). This relatively modest reduction in protein levels is consistent with the known exquisite sensitivity of cells to reduced levels of α -tubulin protein. Diploid *S. cerevisiae* cells are not viable with a single *TUB1* allele (27, 39). Due to the contribution of *TUB3*, such cells have been predicted to contain 60% of the wild-type level of α -tubulin protein (27, 39).

***cef1-13* cells progress through mitosis when the single intron is removed from *TUB1*.** If the *cef1-13* arrest phenotype arises, in whole or in part, because the *TUB1* pre-mRNA is not properly spliced, then removing the *TUB1* intron in the *cef1-13* strain should rescue all or some of the its phenotypes. To test this prediction, an intronless *TUB1* allele, designated *tub1 Δ i*, was created by precisely deleting the single intron from *TUB1* (see Materials and Methods). The genomic copies of *TUB1* were replaced with *tub1 Δ i* in wild-type and *cef1-13* cells (see Material and Methods) to create the *tub1 Δ i* and *cef1-13 tub1 Δ i* strains. Removing the *tub1 Δ i* intron did not alter colony-forming efficiency (data not shown), cell cycle progression (Fig. 4A), or growth (Fig. 4B).

To determine if removing the intron from *TUB1* alters its expression, quantitative Northern blotting was conducted on RNA from wild-type, *tub1 Δ i*, *cef1-13*, and *cef1-13 tub1 Δ i* cells following synchronization and release to the restrictive temperature (Fig. 3B and C). *TUB1* expression was similar between wild-type and *tub1 Δ i* strains at all time points analyzed. As stated previously and consistent with the *cef1-13* intron microarray profile, *cef1-13* cells contained roughly half the amount of *TUB1* message that wild-type cells had, and removing the *TUB1* intron restored expression of *TUB1* in *cef1-13* cells to near wild-type levels (Fig. 3B and C). Specifically, at each time point there was a >79% increase in *TUB1* expression following removal of its intron. Further, the level of α -tubulin protein was restored to the level seen in wild-type cells when the *TUB1* intron was removed from *cef1-13* cells (Fig. 3D). These data indicate that the decrease in *TUB1* expression observed in *cef1-13* cells requires the presence of the *TUB1* intron.

To demonstrate that removing the *TUB1* intron does not restore expression of another intron-containing gene, we analyzed expression of the intron-containing *TUB3* transcript. *TUB3* levels were equivalent in wild-type and *tub1 Δ i* cells but decreased by approximately 50% in both of the *cef1-13* and *cef1-13 tub1 Δ i* strains (Fig. 3B and C). Lastly, we analyzed expression of the *TUB2* transcript, which does not contain an intron. *TUB2* expression was roughly equivalent between all strains at both time points analyzed (Fig. 3B and C), with the notable exception being that arrested *cef1-13 tub1 Δ i* cells displayed decreased expression. Since *TUB2* expression peaks in G₂ (45) and *cef1-13 tub1 Δ i* cells arrest in late mitosis and G₁/S

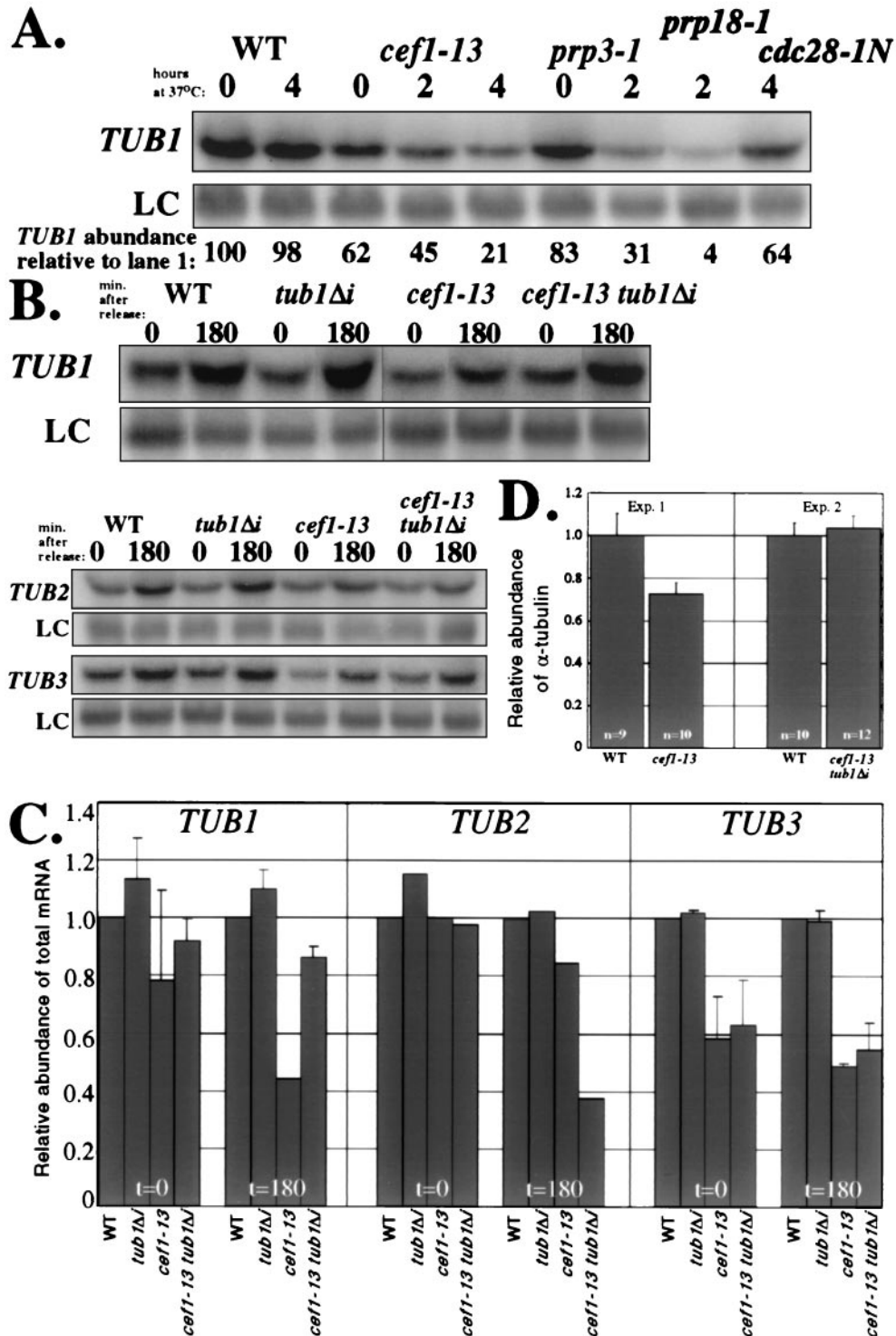


FIG. 3. *cef1-13* cells have less *TUB1* mRNA and α -tubulin protein unless the *TUB1* intron is deleted. (A) Northern analysis of total *TUB1* mRNA abundance in asynchronous cultures shifted to the restrictive temperature. Total RNA was prepared from wild-type (WT), *cef1-13*, *prp3-1*, *prp18-1*, and *cdc28-1N* cells incubated at the permissive temperature or following shift to the restrictive temperature for the indicated number of hours. The levels of *TUB1* mRNA in each sample were quantified by Northern blot analysis using a probe to the entire open reading frame of *TUB1*. The *TUB1* signal in each lane was normalized to that of the non-intron-containing loading control *TDH2* (LC) and expressed as a percentage of *TUB1* in the first lane. (B) Northern analysis of total *TUB1*, *TUB2*, and *TUB3* mRNA abundance following synchronization in G₁ and release to the restrictive temperature. Total RNA was prepared from WT, *tub1Δi*, *cef1-13*, and *cef1-13 tub1Δi* cells 0 and 180 min following release and blotted with probes for the entire open reading frames for *TUB1*, *TUB2*, and *TUB3*. The non-intron-containing *TDH2* transcript was used as an LC. (C) Quantification of Northern analysis shown in panel B. The levels of *TUB* mRNAs in panel B were normalized to that of the LC *TDH2* and expressed as a proportion of lane 1. The relative amounts of each transcript are shown for each strain according to the time point following

(see below), it would be predicted that these cells would contain *TUB2* mRNA in lower abundance.

Next, we evaluated whether removing the *TUB1* intron would alter the arrest phenotype of *cef1-13* cells. Wild type, *tub1* Δ i, *cef1-13*, and *cef1-13 tub1* Δ i strains were synchronized in G_1 with α -factor and released to the restrictive temperature. Following their release, all four strains completed a full round of DNA replication (Fig. 4A). Subsequently, wild-type and *tub1* Δ i cells progressed into the next cell cycle with identical kinetics (Fig. 4A). Following release from G_1 and completion of DNA replication, *cef1-13* cells remained arrested at G_2/M (Fig. 4A). In contrast, *cef1-13 tub1* Δ i cells did not arrest homogeneously in G_2/M but instead progressed into the next cell cycle as evidenced by the reappearance of a G_1 peak later in the time course (Fig. 4A). Cell number determinations made throughout the time course indicated that removing the *TUB1* intron allowed more *cef1-13* cells to undergo cell division (at 3 h, *cef1-13* and *cef1-13 tub1* Δ i had undergone 0.35 and 0.80 doublings, respectively). The cell number (Fig. 4B) and DNA content profiles (data not shown) for the *cef1-13 tub1* Δ i strain were identical at 3 and 4 h, indicating that a terminal arrest phenotype had been reached within 3 h. Analysis of the arrest phenotype for *cef1-13 tub1* Δ i cells confirmed that removing the *TUB1* intron allowed *cef1-13* cells to progress through mitosis (Table 2). Whereas the majority of *cef1-13* cells arrested as large-budded cells with a single nucleus, the majority of *cef1-13 tub1* Δ i arrested as unbudded, small-budded, and large-budded cells with two nuclei. The predominant phenotype present in *cef1-13* cells was not highly represented in the *cef1-13 tub1* Δ i population (Table 2), demonstrating that removal of the *TUB1* intron allowed *cef1-13* cells to undergo anaphase and proceed into the next cell cycle.

That *cef1-13 tub1* Δ i cells were progressing further into the cell cycle was confirmed biochemically by analyzing the levels of Clb2p and Clb2p-associated H1 kinase activity. In contrast to *cef1-13* cells, which arrested with high levels of Clb2p and its associated kinase activity, *cef1-13 tub1* Δ i cells contained low levels of both, indicative of cells that have progressed through mitosis (Fig. 4D) (61). Removing the *TUB1* intron from *cef1-13* cells did not decrease the restrictive temperature for *cef1-13* (data not shown), but it did restore the viability of *cef1-13* cells to near wild-type levels (90% for *cef1-13 tub1* Δ i versus 45% for *cef1-13* at 3 h following release from α -factor). Taken together, these data demonstrate that *cef1-13* cells arrest prior to anaphase in large measure because the *TUB1* mRNA levels become limiting, probably due to inefficient pre-mRNA splicing.

Based on the bud and nuclear morphologies, we predicted that, contrary to *cef1-13* cells, *cef1-13 tub1* Δ i cells should contain stable microtubules. To confirm this, we visualized α -tubulin in wild-type, *tub1* Δ i, *cef1-13*, and *cef1-13 tub1* Δ i cells by indirect immunofluorescence 2 h following release from α -fac-

tor. Wild-type and *tub1* Δ i cells displayed indistinguishable microtubule arrays (data not shown). Consistent with previous experiments, *cef1-13* cells did not display visible microtubule structures, whereas *cef1-13 tub1* Δ i cells contained normal microtubule structures including spindles (Fig. 4C).

Lastly, we determined what effect removing the *TUB1* intron would have on *cef1-13* cell benomyl sensitivity. Wild-type, *tub1* Δ i, *cef1-13*, and *cef1-13 tub1* Δ i cells were plated on agar plates containing increasing concentrations of benomyl. The *tub1* Δ i strain formed an equal number of colonies to the wild-type strain at each concentration (Fig. 4E). Removing the *TUB1* intron in *cef1-13* cells modestly increased this strain's resistance to benomyl (Fig. 4E). These data indicate that inefficient splicing of *TUB1* contributes to the *cef1-13* strain's sensitivity to benomyl. The residual benomyl sensitivity in *cef1-13 tub1* Δ i cells is likely a function of reduced *TUB3* and *GIM5* mRNAs. Although neither of these genes is essential, mutations in either cause hypersensitivity to benomyl (16, 40).

An alternative explanation for the suppression of the *cef1-13* cell cycle arrest is that removing the *TUB1* intron decreases demand on the splicing machinery. To test this, we created a *cef1-13* strain that lacked the intron for another gene, *SAR1*. The *SAR1* mRNA is present at a greater copy number per cell than the *TUB1* mRNA and is transcribed at a greater rate (5.8 or 2.6 copies per cell and 15.1 or 6.1 mRNAs/h for *SAR1* and *TUB1*, respectively [23]). Following synchronous release to the restrictive temperature, *cef1-13 sar1* Δ i cells displayed growth characteristics and a G_2/M arrest phenotype matching those of *cef1-13* cells (data not shown). Furthermore, removing the *TUB1* intron allowed *cef1-13* cells to segregate their nuclei, whereas removing the *SAR1* intron did not (Table 4). These data indicate that removing the *SAR1* intron did not allow *cef1-13* cells to progress through mitosis, demonstrating that the effect of removing the *TUB1* intron is specific.

An extra copy of wild-type *TUB1* allows *cef1-13* cells to progress through mitosis. If inefficient splicing of *TUB1* causes the *cef1-13* phenotype, then it would be predicted that, like removing the *TUB1* intron, introducing an extra copy of the wild-type *TUB1* gene into *cef1-13* cells might allow progression through mitosis. To test this prediction, wild-type and *cef1-13* cells were transformed with three plasmids: an empty *CEN* vector (pRS415), the same vector containing the wild-type *TUB1* gene (pRS415*TUB1*), or the same vector containing the intronless *tub1* Δ i allele (pRS415*tub1* Δ i). All six transformants were synchronized and released to the restrictive temperature. The three wild-type transformants were indistinguishable with respect to cell number (data not shown), cell cycle progression (data not shown), and bud and nuclear morphologies (Table 5). As expected, the *cef1-13* strain carrying the empty vector arrested in the first cell cycle with a minimal increase in cell number (Fig. 5), homogenous arrest in G_2/M (Fig. 5), and a

release from G_1 . (D) Examination of α -tubulin protein in *cef1-13* strains. WT, *cef1-13*, and *cef1-13 tub1* Δ i cells were synchronized with mating pheromone and released to the restrictive temperature. At 180 min following release, multiple pellets (optical density = 10) were collected. Strains for each experiment were prepared twice. Protein lysates were made from each pellet, and bicinchoninic assays were conducted to allow normalization of protein concentrations between all samples. Equivalent amounts of protein were blotted with an α -tubulin monoclonal antibody (α) and polyclonal antisera raised against TATA-binding protein (encoded by a non-intron-containing gene) as a loading control. The immunoblots were quantitated using a Molecular Dynamics Storm instrument, and the results of α -tubulin protein relative to TATA-binding protein were graphed. The bars indicate the average and standard deviation (error bars). The number of independent analyses for each strain is indicated.

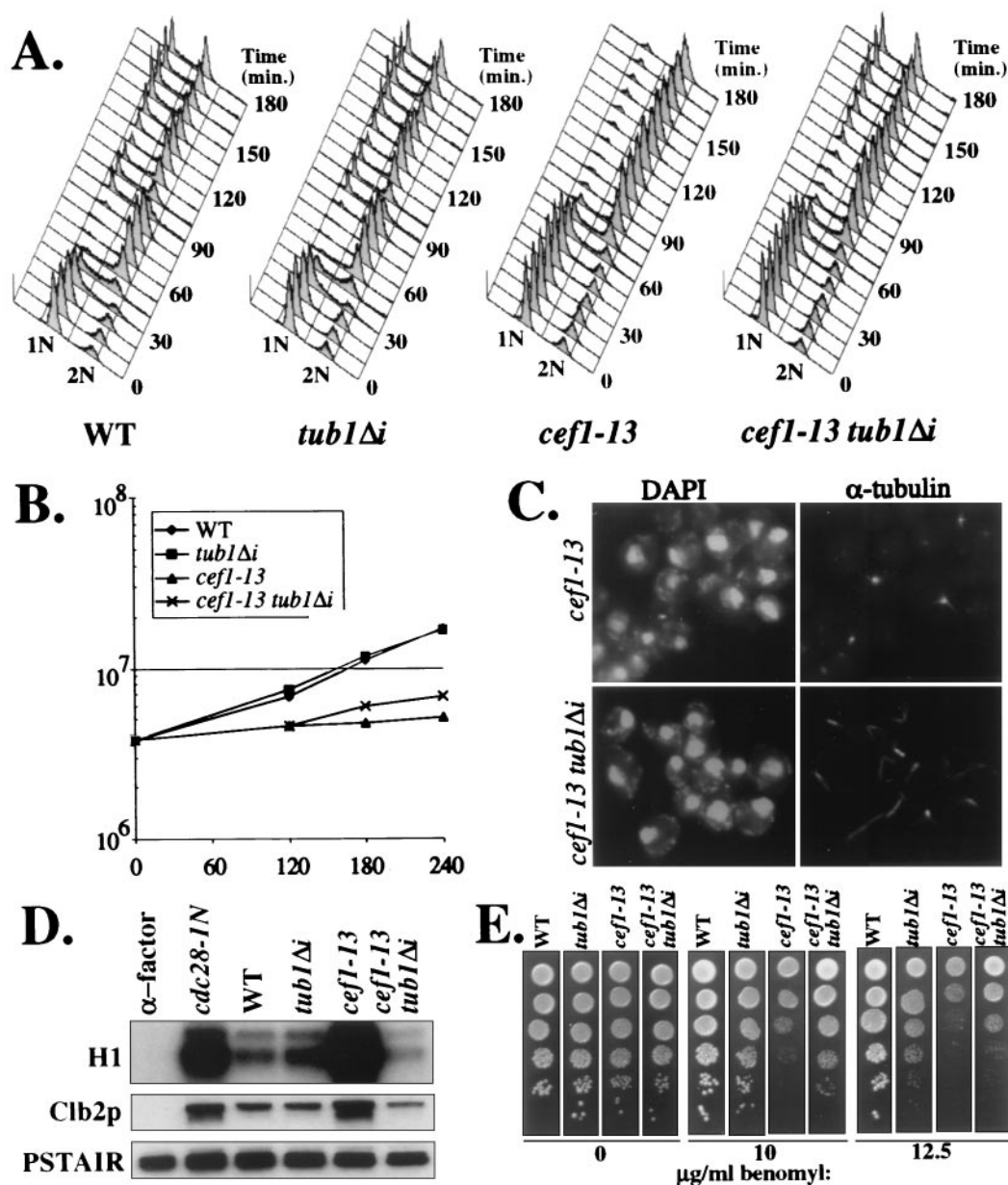








FIG. 4. Removing the intron from *TUB1* allows *cef1-13* cells to progress through mitosis. Wild-type (WT), *tub1Δi*, *cef1-13*, and *cef1-13 tub1Δi* cells were synchronized in G_1 with α -factor and released to the restrictive temperature. Following their release, cultures were monitored for cell number (B) and cell cycle progression as reflected by DNA content (A). (C) At 2 h following release, the status of microtubule structures in *cef1-13* and *cef1-13 tub1Δi* cells was evaluated with indirect immunofluorescence. (D) At 3 h following release, the levels of the mitotic cyclin Clb2p and its associated H1 kinase activity were evaluated. G_1 -arrested WT cells and G_2/M -arrested *cdc28-1N* cells were used as controls for low and high Clb2p and kinase activity, respectively. G_1 -arrested cells were obtained by treating WT cells with α -factor. G_2/M -arrested cells were obtained by synchronizing *cdc28-1N* cells with α -factor and releasing them to the restrictive temperature for 3 h. (E) Tenfold serial dilutions of WT, *tub1Δi*, *cef1-13*, and *cef1-13 tub1Δi* cells were spotted on YPD agar with the indicated concentrations of benomyl and incubated at 25°C for 3 days prior to being photographed.

predominance of large-budded cells with a single nucleus (Table 5). In contrast, *cef1-13* cells carrying the wild-type *TUB1* allele were able to reenter the next cell cycle as evidenced by the reappearance of a G_1 peak late in the time course (Fig. 5). Furthermore, these cells displayed a greater increase in cell number (Fig. 5) and a disappearance of the large-budded phenotype compared to *cef1-13* cells carrying the empty vector (Table 5). These data indicate that an extra copy of *TUB1* alone will allow *cef1-13* cells to progress through mitosis.

cef1-13 cells carrying the plasmid-borne *tub1Δi* allele were similarly able to progress through mitosis (Fig. 5; Table 5). These cells showed the greatest increase in cell number of all of the *cef1-13* strains, which indicates that the intronless *tub1Δi* allele is more efficient than the wild-type allele at allowing mitotic progression in these conditions.

Removing the intron from *TUB1* allows *prp17* and *prp22* mutants to segregate their nuclei. To determine if other *prp* mutants that arrest at G_2/M do so because of a failure to splice

TABLE 4. Quantitation of cell and nuclear morphologies 180 min following release from α -factor

Cell	% of total cells displaying indicated morphology ^a						Other	<i>n</i> ^b
								
Wild type	52	26	3	0	3	14	1	400
<i>cef1-13</i>	22	13	36	14	2	5	9	400
<i>cef1-13 tub1Δi</i>	52	18	2	1	5	20	4	400
<i>cef1-13 sar1Δi</i>	30	15	29	11	3	8	5	400







^a Each morphologic class is shown schematically. Large-budded cells were scored if the bud was equal to or greater than half of the size of the mother. The percentages do not always add up to 100% due to rounding.

^b *n*, total number of cells counted.

TUB1 pre-mRNAs, we evaluated the effects of removing the *TUB1* intron from temperature-sensitive mutants of *prp17* (56) and *prp22* (24, 57), the only other splicing mutants reported to arrest at G₂/M. *PRP17* encodes a protein involved in the second catalytic step of the splicing reaction, and the temperature-sensitive *prp17*-null (*prp17Δ*) cells arrest at G₂/M without microtubules (56). *PRP22* encodes a DEAH box protein required for mRNA release from the spliceosome (58), and temperature-sensitive alleles of *PRP22* were identified in a screen for mutants that arrest in mitosis (24).

We removed the *TUB1* intron from the genomic *TUB1* locus in *prp17Δ* and *prp22-1* mutants to determine if, as for *cef1-13*, the intronless *TUB1* would allow for progression through mitosis. These cells (along with their isogenic *TUB1* intron-containing counterparts) were synchronized in G₁ with α -factor and released to the restrictive temperature. Cell numbers were essentially constant throughout the course of the experiment for all four mutant strains (Fig. 6). Following DNA replication, all of the mutant strains arrested predominantly with a 2*N* content of DNA, although a small G₁ peak reappeared in the *prp22-1 tub1Δi* strain (Fig. 6). Analysis of bud and nuclear morphologies 3 h following release revealed that like *cef1-13* cells, *prp17Δ* and *prp22-1* cells arrested with a significant per-

TABLE 5. Quantitation of cell and nuclear morphologies 180 min following release from α -factor

Cell	% of total cells displaying indicated morphology ^a						Other	<i>n</i> ^b
								
WT ^c + pRS415	27	38	7	0	9	19	1	399
WT + pRS415 <i>TUB1</i>	28	37	4	0	11	20	1	399
WT + pRS415 <i>tub1Δi</i>	32	34	3	0	11	19	1	400
<i>cef1-13</i> + pRS415	13	14	43	20	3	4	3	399
<i>cef1-13</i> + pRS415 <i>TUB1</i>	21	17	16	3	12	27	6	400
<i>cef1-13</i> + pRS415 <i>tub1Δi</i>	28	14	13	3	16	22	6	400

^a Each morphologic class is shown schematically. Large-budded cells were scored if the bud was equal to or greater than half of the size of the mother. The percentages do not always add up to 100% due to rounding.

^b *n*, total number of cells counted.

^c WT, wild type.

centage of large-budded cells with a single nucleus (Table 6). Removing the *TUB1* intron from either mutant decreased the percentage of cells with this arrest phenotype and increased the percentage of large-budded cells with segregated nuclei (Table 6). These data indicate that removing the *TUB1* intron from two other splicing mutants allowed for nuclear division. Therefore, inefficient splicing of *TUB1* can explain in part or in full why certain splicing mutants arrest with unsegregated chromosomes.

DISCUSSION

Pre-mRNA splicing and cell cycle control have independent functions for eukaryotic cells. However, these processes might be linked, because yeast proteins have been identified through genetic criteria as splicing factors and independently as essential for cell cycle progression (10). The conserved Myb-related CDC5/Cef1p proteins carry essential functions in both processes, because their genetic depletion in the fission (30) and budding (11) yeasts causes accumulation of pre-mRNAs and cell cycle arrest at G₂/M. Through characterization of a novel temperature-sensitive allele of *S. cerevisiae* *CEF1*, *cef1-13*, we have demonstrated that G₂/M cell cycle arrest results from inefficient splicing of the *TUB1* pre-mRNA that encodes the major yeast α -tubulin. *TUB1* intron deletion also partially suppresses the G₂/M arrest observed in mutants of the splicing proteins Prp17p and Prp22p.

cef1-13 cells arrest homogeneously in G₂/M prior to the first encountered anaphase when released to the restrictive temperature as a synchronous culture from G₁. The arrest phenotype includes many features indicative of defects in microtubules: nuclear positioning defects, depolymerization of microtubules upon chemical fixation, and benomyl sensitivity (41). Because CDC5/Cef1p proteins have been implicated in pre-mRNA splicing, we hypothesized that the *cef1-13* phenotype might arise because a specific nascent transcript was not processed efficiently at the restrictive temperature.

We used splicing-sensitive oligonucleotide microarrays to search for those transcripts not spliced efficiently in *cef1-13* cells and whose inefficient splicing might account for the G₂/M arrest phenotype. We determined that *cef1-13* was generally defective in pre-mRNA splicing, confirming the conclusion that *CEF1* is a bona fide splicing factor (1, 11, 53). Furthermore, of essential transcripts, *TUB1* was the most affected. Despite the fact that *cef1-13* cells contained higher levels of the *TUB1* precursor as detected with the microarrays, we did not detect a temperature-dependent accumulation of this species in *cef1-13* cells by Northern analysis (data not shown). This feature of the *cef1-13* phenotype is common among splicing mutants. Many pre-mRNAs do not accumulate in temperature-sensitive splicing mutants despite a strong reduction in mRNA levels, because the precursors are degraded by a pathway for nuclear pre-mRNA turnover (8).

Despite the general defect in splicing, our attention was drawn to the *TUB1* gene. Of essential intron-containing transcripts, the microarray analysis indicated that *TUB1* was the most affected in *cef1-13* cells. *TUB1* encodes the major α -tubulin protein in *S. cerevisiae*, and *tub1* mutants can display phenotypes similar to those of *cef1-13* cells, including unstable microtubules, nuclear positioning defects, and G₂/M arrest

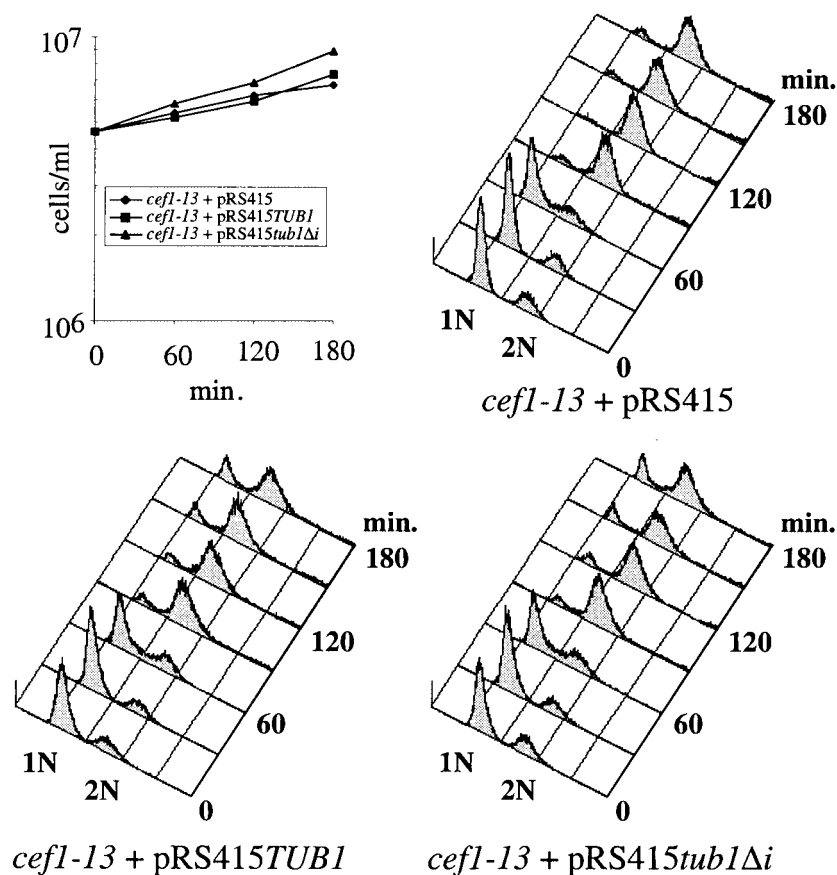


FIG. 5. An extra copy of *TUB1* allows *cef1-13* cells to progress through mitosis. *cef1-13* cells carrying an empty *CEN* vector or the same vector containing the wild-type *TUB1* allele or the intronless *tub1* Δ i allele were synchronized in G_1 and released to the restrictive temperature. Released cultures were monitored for cell number (upper left) and cell cycle progression as reflected by DNA content.

(39–41). Therefore, we tested the hypothesis that inefficient splicing of *TUB1* was responsible for the cell cycle phenotypes displayed by *cef1-13* cells.

Uncoupling the production of mature *TUB1* mRNA from splicing of its pre-mRNA was accomplished by removing the single intron from the genomic *TUB1* locus. Consistent with our hypothesis, removal of the *TUB1* intron allowed *cef1-13* cells to progress through mitosis, as evidenced by nuclear and cell division. Removing the intron from *TUB1* did not rescue the growth defect of the *cef1-13* strain, indicating that another transcript(s) becomes rate limiting for growth after the cells have passed through mitosis. Removing the intron from another gene, *SARI*, did not alleviate the cell cycle phenotype in *cef1-13* cells, indicating that the effect of removing the *TUB1* intron is specific.

The twofold reduction in total *TUB1* mRNA in *cef1-13* cells at the restrictive temperature translated to a 30% reduction in the steady-state levels of α -tubulin protein. Given that α -tubulin is a stable (4) and moderately abundant (21) protein, it is understandable why decreased synthesis would take generation times to fully manifest itself with an equivalent reduction in the total pool of α -tubulin protein. However, it is not surprising that a modest decrease in α -tubulin protein would have a profound effect on microtubule dynamic instability in vivo and

therefore on cell growth. In *S. cerevisiae*, it has been well established that increasing the ratio of β - to α -tubulin through mutations in the α -tubulin-encoding *TUB1* (40, 41) or overproduction of the β -tubulin-encoding *TUB2* (9, 27, 59) will cause cells to arrest in G_2/M with unstable microtubules, large buds, and single nuclei. Furthermore, diploid cells hemizygous with respect to *TUB1* (these cells would be predicted to contain 60% of α -tubulin levels, with the extra 10% coming from *TUB3* [27]) cannot be isolated without an extra copy of chromosome 13, which carries both *TUB1* and *TUB3* (27, 39). Since the β -tubulin mRNA (encoded by the non-intron-containing *TUB2* gene, see above) and protein levels (data not shown) are unaffected in *cef1-13* cells, the decrease in α -tubulin protein would be predicted to decrease the ratio of α - to β -tubulin and result in several features of the *cef1-13* phenotype. In light of this, it is not surprising that extra copies of intron-containing *TUB1* allowed *cef1-13* cells to progress through mitosis, similar to removal of its intron.

In addition to altering the ratio of β - to α -tubulin, we would predict a significant decrease in the pool of newly synthesized α -tubulin protein in *cef1-13* cells that is presumably unpolymerized. Since the rate of microtubule polymerization in vitro is highly dependent on the concentration of tubulin (14), a reduction in the levels of unpolymerized tubulin could have

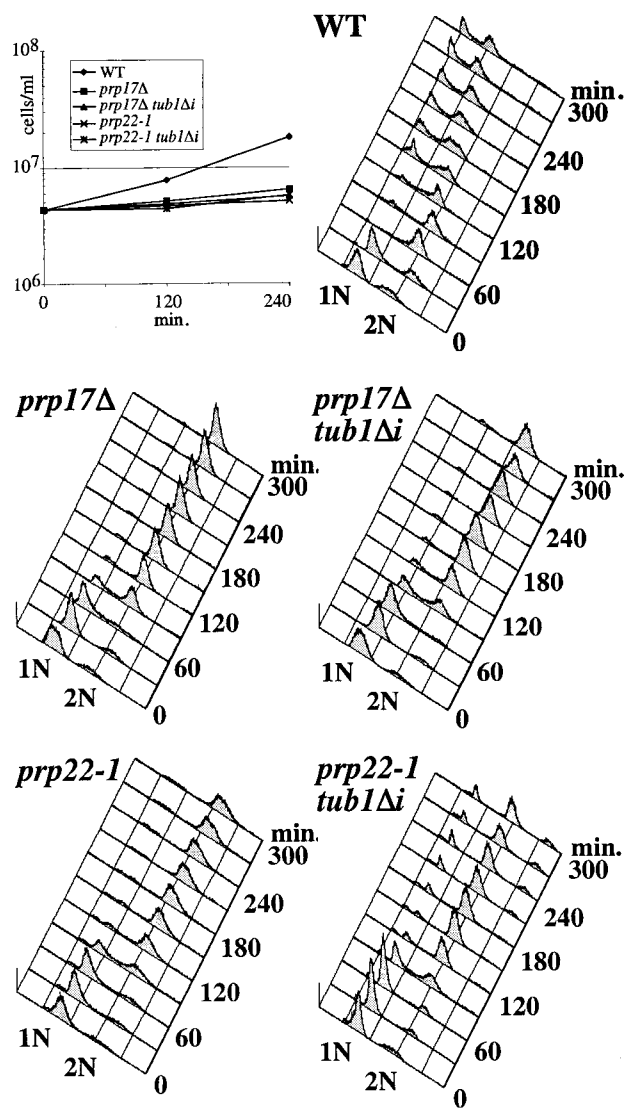


FIG. 6. Cell cycle arrest of *prp17* and *prp22* mutants. Wild-type (WT), *prp17Δ*, *prp17Δtub1Δi*, *prp22-1*, and *prp22-1 tub1Δi* cells were synchronized in G_1 and released to the restrictive temperature. Released cultures were monitored for cell number (upper left) and cell cycle progression as reflected by DNA content.

dramatic consequences on the stability of polymerized microtubules in vivo. Indeed, *cef1-13* cells have unstable microtubules, and removing the intron from *TUB1* restores microtubule stability. Furthermore, because other genes involved in tubulin biogenesis contain introns and are not spliced properly in *cef1-13* cells (such as *GIM5*), it is likely that *cef1-13* cells have a lower tolerance than wild-type cells for a reduction in α -tubulin production. Lastly, our data do not rule out the possibility that an alteration in the production of *TUB1* message directly influences microtubule stability. To our knowledge, however, there are no data in the literature indicating that such a pathway might exist.

In addition to *TUB1*, there are two other intron-containing genes that are known to be important for microtubule func-

TABLE 6. Quantitation of cell and nuclear morphologies 240 min following release from α -factor

Cell	% of total cells displaying indicated morphology ^a							<i>n</i> ^b
							Other	
Wild type	49	26	5	0	2	16	2	400
<i>prp17Δ TUB1</i>	20	36	24	16	4	1	0	400
<i>prp17Δ tub1Δi</i>	20	34	7	5	8	24	1	401
<i>prp22-1 TUB1</i>	25	13	26	27	2	2	6	400
<i>prp22-1 tub1Δi</i>	24	18	8	3	5	38	5	407

^a Each morphologic class is shown schematically. Large-budded cells were scored if the bud was equal to or greater than half of the size of the mother. The percentages do not always add up to 100% due to rounding.

^b *n*, total number of cells counted.

tion: *TUB3*, which encodes the minor α -tubulin (39, 40), and *GIM5*, which encodes a protein that is required for correct folding of tubulin subunits (16). Although neither gene is essential for growth, deletion of either one causes benomyl sensitivity (16, 40, 47). Furthermore, synthetic lethal interactions between *GIM5* and mutations in *TUB1* have been reported (55). Therefore, it is possible that a cell cycle block could be caused by inefficient production of a combination of these different mRNAs. The spliced forms of the mRNAs from *TUB3* and *GIM5* were decreased in the *cef1-13* mutant (Table 3). However, because removal of the *TUB1* intron effectively eliminates a cell cycle phenotype, it is likely that a significant impact of splicing inefficiency on cell cycle progression in *cef1-13* cells is mediated through *TUB1*. In the case of mutations in two other splicing factors, Prp17p and Prp22p, that cause G_2/M arrest (5, 24), we found that removal of the *TUB1* intron allowed increased efficiency of nuclear division and, to a lesser extent, cell division. Suppression may not be as complete in these cases as it is with *cef1-13* if the *prp17* and *prp22* mutations have stronger effects on the processing of *TUB3* and *GIM5*. Whether removal of the introns from these genes in addition to that of *TUB1* will eliminate the cell cycle arrest phenotype of the *prp17* and *prp22* mutants is under investigation.

It is likely that the *CEF1* ortholog in *S. pombe*, *cdc5+*, is also required for splicing the intron-containing α -tubulin gene, *nda2+* (52), in this evolutionarily distinct yeast. The temperature-sensitive *cdc5-120* mutant exhibits sensitivity to the microtubule-destabilizing drug thiabendazole and displays defects in cell polarity when combined with mutations in β -tubulin (R. Ohi and K. L. Gould, unpublished results), both characteristics of defective microtubules in fission yeast. However, because the majority of *cdc5-120* cells arrest prior to entry into mitosis (34), it seems unlikely that reduced expression of the mature *nda2+* transcript is as significant in their arrest phenotype. Compared to *S. cerevisiae*, *S. pombe* contains a greater percentage of genes with introns (approximately 45% [62]), and there are a large number of candidate genes whose inefficient splicing might contribute to the G_2 arrest of *cdc5-120* cells.

To determine whether cell cycle arrest is a common feature of *S. cerevisiae* splicing mutants, we have evaluated the cell cycle phenotypes of 10 splicing mutants (*prp2-1*, *prp3-1*, *prp4-1*, *prp5-1*, *prp17-1*, *prp17/cdc40Δ*, *prp18-1*, *prp19-1*, *prp20-1*, and *prp22-1* strains) following release to the restrictive temperature

from an α -factor block. We found that some mutants display cell cycle phenotypes although they differ, and some mutants arrest heterogeneously throughout the cell cycle (C. G. Burns and K. L. Gould, unpublished results). Only mutations in *PRP17* and *PRP22* caused a first cell cycle arrest in G_2/M .

The source of variability in the timing of arrest and appearance of cell cycle phenotypes among splicing mutants is unclear. The cell cycle defect (or lack thereof) might be a function of the severity of the splicing defect. For instance, mutants that arrest early after release from a G_1 block might have a more severe splicing defect than those that arrest later or continue to undergo one or two divisions and arrest without a homogeneous phenotype. An alternative explanation would be that protein factors are differentially required for efficient processing of single transcripts or a subset of transcripts. If this is true, then multiple rate-limiting transcripts (and, therefore, cell cycle phenotypes) would arise from mutating different splicing factors. For example, it is possible that *CEF1*, *PRP17*, and *PRP22* have more important roles in splicing transcripts critical for G_2/M progression and that is why mutations in these proteins cause G_2/M arrest. That protein factors perform specialized roles in splicing specific transcripts would be analogous to the role of the TAF proteins in regulating transcription. Of the TAF proteins in *S. cerevisiae*, yTAF145, TSM1, and yTAF90 are required for transcriptional activation of a subset of genes necessary for cell cycle progression (2, 3, 23, 60). A complete list of transcriptional targets for many of the TAFs has been identified through genome-wide expression analysis of TAF mutants (23). A similar approach would be valuable to determine if protein factors play specialized roles in pre-mRNA splicing and which transcripts require specialized regulation.

ACKNOWLEDGMENTS

We thank K. Gull, D. C. Kaiser, D. Kellogg, J. Patton, S. Reed, B. Rymond, and P. A. Weil for their generous gifts of strains, plasmids, and antibodies. We are grateful to D. McFarland and Michelle Thornsberry for flow cytometric analysis. Mary Morphey (Boulder Laboratory for 3D Fine Structure) kindly prepared specimens for electron micrograph analysis. J. Flick and all members of the Gould laboratory are acknowledged for providing useful discussions.

This work was supported by NIH grant GM47728 to K.L.G. Microarray work was supported by a grant from the W. M. Keck Foundation to the RNA Center at the University of California at Santa Cruz. C.G.B. was supported by NIH Medical Scientist Training Program grant GM07347. K.L.G. is an Associate Investigator of the Howard Hughes Medical Institute.

REFERENCES

- Ajuh, P., B. Kuster, K. Panov, J. C. Zomerdijk, M. Mann, and A. I. Lamond. 2000. Functional analysis of the human CDC5L complex and identification of its components by mass spectrometry. *EMBO J.* **19**:6569–6581.
- Albright, S. R., and R. Tjian. 2000. TAFs revisited: more data reveal new twists and confirm old ideas. *Gene* **242**:1–13.
- Apone, L. M., C. M. Virbasius, J. C. Reese, and M. R. Green. 1996. Yeast TAF(II)90 is required for cell-cycle progression through G_2/M but not for general transcription activation. *Genes Dev.* **10**:2368–2380.
- Archer, J. E., L. R. Vega, and F. Solomon. 1995. Rbl2p, a yeast protein that binds to beta-tubulin and participates in microtubule function in vivo. *Cell* **82**:425–434.
- Ben-Yehuda, S., I. Dix, C. S. Russell, M. McGarvey, J. D. Beggs, and M. Kupiec. 2000. Genetic and physical interactions between factors involved in both cell cycle progression and pre-mRNA splicing in *Saccharomyces cerevisiae*. *Genetics* **156**:1503–1517.
- Bernstein, H. S., and S. R. Coughlin. 1998. A mammalian homolog of fission yeast Cdc5 regulates G_2 progression and mitotic entry. *J. Biol. Chem.* **273**:4666–4671.
- Bernstein, H. S., and S. R. Coughlin. 1997. Pombe Cdc5-related protein. A putative human transcription factor implicated in mitogen-activated signaling. *J. Biol. Chem.* **272**:5833–5837.
- Bousquet-Antonelli, C., C. Presutti, and D. Tollervey. 2000. Identification of a regulated pathway for nuclear pre-mRNA turnover. *Cell* **102**:765–775.
- Burke, D., P. Gasdaska, and L. Hartwell. 1989. Dominant effects of tubulin overexpression in *Saccharomyces cerevisiae*. *Mol. Cell. Biol.* **9**:1049–1059.
- Burns, C. G., and K. L. Gould. 1999. Connections between pre-mRNA processing and regulation of the eukaryotic cell cycle, p. 59–82. *In* S. L. Chew (ed.), *Post-transcriptional regulation of gene expression and its importance to the endocrine system*, vol. 25. Karger, Basel, Switzerland.
- Burns, C. G., R. Ohi, A. R. Krainer, and K. L. Gould. 1999. Evidence that Myb-related CDC5 proteins are required for pre-mRNA splicing. *Proc. Natl. Acad. Sci. USA* **96**:13789–13794.
- Chen, E. J., A. R. Frand, E. Chitouras, and C. A. Kaiser. 1998. A link between secretion and pre-mRNA processing defects in *Saccharomyces cerevisiae* and the identification of a novel splicing gene, *RSE1*. *Mol. Cell. Biol.* **18**:7139–7146.
- Davis, C. A., L. Grate, M. Spingola, and M. Ares, Jr. 2000. Test of intron predictions reveals novel splice sites, alternatively spliced mRNAs and new introns in meiotically regulated genes of yeast. *Nucleic Acids Res.* **28**:1700–1706.
- Desai, A., and T. J. Mitchison. 1997. Microtubule polymerization dynamics. *Annu. Rev. Cell Dev. Biol.* **13**:83–117.
- Epstein, C. B., and F. R. Cross. 1992. CLB5: a novel B cyclin from budding yeast with a role in S phase. *Genes Dev.* **6**:1695–1706.
- Geissler, S., K. Siegers, and E. Schiebel. 1998. A novel protein complex promoting formation of functional alpha- and gamma-tubulin. *EMBO J.* **17**:952–966.
- Giddings, T. H. J., E. T. O'Toole, M. Morphey, D. N. Mastrorade, J. R. McIntosh, and M. Winey. 2001. Using rapid freeze and freeze-substitution for the preparation of yeast cells for electron microscopy and three-dimensional analysis. *Methods Cell Biol.* **67**:27–42.
- Groenen, P. M., G. Vanderlinden, K. Devriendt, J. P. Fryns, and W. J. Van de Ven. 1998. Rearrangement of the human CDC5L gene by a t(6;19)(p21;q13.1) in a patient with multicystic renal dysplasia. *Genomics* **49**:218–229.
- Gui, J. F., W. S. Lane, and X. D. Fu. 1994. A serine kinase regulates intracellular localization of splicing factors in the cell cycle. *Nature* **369**:678–682.
- Guthrie, C., and G. R. Fink (ed.). 1991. *Methods in enzymology*, vol. 194. Guide to yeast genetics and molecular biology. Academic Press, San Diego, Calif.
- Gygi, S. P., Y. Rochon, B. R. Franza, and R. Aebersold. 1999. Correlation between protein and mRNA abundance in yeast. *Mol. Cell. Biol.* **19**:1720–1730.
- Hirayama, T., and K. Shinozaki. 1996. A cdc5+ homolog of a higher plant, *Arabidopsis thaliana*. *Proc. Natl. Acad. Sci. USA* **93**:13371–13376.
- Holstege, F. C., E. G. Jennings, J. J. Wyrick, T. I. Lee, C. J. Hengartner, M. R. Green, T. R. Golub, E. S. Lander, and R. A. Young. 1998. Dissecting the regulatory circuitry of a eukaryotic genome. *Cell* **95**:717–728.
- Hwang, L. H., and A. W. Murray. 1997. A novel yeast screen for mitotic arrest mutants identifies DOC1, a new gene involved in cyclin proteolysis. *Mol. Biol. Cell* **8**:1877–1887.
- Ito, H., Y. Fukuda, K. Murata, and A. Kimura. 1983. Transformation of intact yeast cells treated with alkali cations. *J. Bacteriol.* **153**:163–168.
- Johnston, L. H., and A. P. Thomas. 1982. The isolation of new DNA synthesis mutants in the yeast *Saccharomyces cerevisiae*. *Mol. Gen. Genet.* **186**:439–444.
- Katz, W., B. Weinstein, and F. Solomon. 1990. Regulation of tubulin levels and microtubule assembly in *Saccharomyces cerevisiae*: consequences of altered tubulin gene copy number. *Mol. Cell. Biol.* **10**:5286–5294.
- Kellogg, D. R., and A. W. Murray. 1995. NAP1 acts with Clb1 to perform mitotic functions and to suppress polar bud growth in budding yeast. *J. Cell Biol.* **130**:675–685.
- Lundgren, K., S. Allan, S. Urushiyama, T. Tani, Y. Ohshima, D. Frendewey, and D. Beach. 1996. A connection between pre-mRNA splicing and the cell cycle in fission yeast: cdc28+ is allelic with prp8+ and encodes an RNA-dependent ATPase/helicase. *Mol. Biol. Cell* **7**:1083–1094.
- McDonald, W. H., R. Ohi, N. Smelkova, D. Frendewey, and K. L. Gould. 1999. Myb-related fission yeast cdc5p is a component of a 40S snRNP-containing complex and is essential for pre-mRNA splicing. *Mol. Cell. Biol.* **19**:5352–5362.
- Neubauer, G., A. King, J. Rappsilber, C. Calvio, M. Watson, P. Ajuh, J. Sleeman, A. Lamond, and M. Mann. 1998. Mass spectrometry and EST-database searching allows characterization of the multi-protein spliceosome complex. *Nat. Genet.* **20**:46–50.
- Nurse, P., P. Thuriaux, and K. Nasmyth. 1976. Genetic control of the cell division cycle in the fission yeast *Schizosaccharomyces pombe*. *Mol. Gen. Genet.* **146**:167–178.
- Ohi, R., A. Feoktistova, S. McCann, V. Valentine, A. T. Look, J. S. Lipsick, and K. L. Gould. 1998. Myb-related *Schizosaccharomyces pombe* cdc5p is

- structurally and functionally conserved in eukaryotes. *Mol. Cell. Biol.* **18**:4097–4108.
34. **Ohi, R., D. McCollum, B. Hirani, G. J. Den Haese, X. Zhang, J. D. Burke, K. Turner, and K. L. Gould.** 1994. The *Schizosaccharomyces pombe* *cdc5+* gene encodes an essential protein with homology to c-Myb. *EMBO J.* **13**:471–483.
 35. **Poon, D., and P. A. Weil.** 1993. Immunopurification of yeast TATA-binding protein and associated factors. Presence of transcription factor IIIB transcriptional activity. *J. Biol. Chem.* **268**:15325–15328.
 36. **Potashkin, J., D. Kim, M. Fons, T. Humphrey, and D. Frendewey.** 1998. Cell-division-cycle defects associated with fission yeast pre-mRNA splicing mutants. *Curr. Genet.* **34**:153–163.
 37. **Pringle, J., A. E. M. Adams, D. G. Drubin, and B. K. Haarer.** 1991. Immunofluorescence methods for yeast, p. 565–601. *In* C. Guthrie and G. R. Fink (ed.), *Guide to yeast genetics and molecular biology*. Academic Press, San Diego, Calif.
 38. **Reed, S. L., J. A. Hadwiger, and A. T. Lorincz.** 1985. Protein kinase activity associated with the product of the yeast cell division cycle gene *CDC28*. *Proc. Natl. Acad. Sci. USA* **82**:4055–4059.
 39. **Schatz, P. J., L. Pillus, P. Grisafi, F. Solomon, and D. Botstein.** 1986. Two functional alpha-tubulin genes of the yeast *Saccharomyces cerevisiae* encode divergent proteins. *Mol. Cell. Biol.* **6**:3711–3721.
 40. **Schatz, P. J., F. Solomon, and D. Botstein.** 1986. Genetically essential and nonessential alpha-tubulin genes specify functionally interchangeable proteins. *Mol. Cell. Biol.* **6**:3722–3733.
 41. **Schatz, P. J., F. Solomon, and D. Botstein.** 1988. Isolation and characterization of conditional-lethal mutations in the *TUB1* alpha-tubulin gene of the yeast *Saccharomyces cerevisiae*. *Genetics* **120**:681–695.
 42. **Scherer, S., and R. W. Davis.** 1979. Replacement of chromosome segments with altered DNA sequences constructed in vitro. *Proc. Natl. Acad. Sci. USA* **76**:4951–4955.
 43. **Seghezzi, W., K. Chua, F. Shanahan, O. Gozani, R. Reed, and E. Lees.** 1998. Cyclin E associates with components of the pre-mRNA splicing machinery in mammalian cells. *Mol. Cell. Biol.* **18**:4526–4536.
 44. **Shea, J. E., J. H. Toyn, and L. H. Johnston.** 1994. The budding yeast U5 snRNP Prp8 is a highly conserved protein which links RNA splicing with cell cycle progression. *Nucleic Acids Res.* **22**:5555–5564.
 45. **Spellman, P. T., G. Sherlock, M. Q. Zhang, V. R. Iyer, K. Anders, M. B. Eisen, P. O. Brown, D. Botstein, and B. Futcher.** 1998. Comprehensive identification of cell cycle-regulated genes of the yeast *Saccharomyces cerevisiae* by microarray hybridization. *Mol. Biol. Cell* **9**:3273–3297.
 46. **Spingola, M., L. Grate, D. Haussler, and M. Ares, Jr.** 1999. Genome-wide bioinformatic and molecular analysis of introns in *Saccharomyces cerevisiae*. *RNA* **5**:221–234.
 47. **Stearns, T., M. A. Hoyt, and D. Botstein.** 1990. Yeast mutants sensitive to antimicrotubule drugs define three genes that affect microtubule function. *Genetics* **124**:251–262.
 48. **Stukenberg, P. T., K. D. Lustig, T. J. McGarry, R. W. King, J. Kuang, and M. W. Kirschner.** 1997. Systematic identification of mitotic phosphoproteins. *Curr. Biol.* **7**:338–348.
 49. **Takahashi, K., H. Yamada, and M. Yanagida.** 1994. Fission yeast minichromosome loss mutants mis cause lethal aneuploidy and replication abnormality. *Mol. Biol. Cell* **5**:1145–1158.
 50. **Tang, Z., M. Yanagida, and R. J. Lin.** 1998. Fission yeast mitotic regulator Dsk1 is an SR protein-specific kinase. *J. Biol. Chem.* **273**:5963–5969.
 51. **Tarn, W. Y., C. H. Hsu, K. T. Huang, H. R. Chen, H. Y. Kao, K. R. Lee, and S. C. Cheng.** 1994. Functional association of essential splicing factor(s) with PRP19 in a protein complex. *EMBO J.* **13**:2421–2431.
 52. **Toda, T., Y. Adachi, Y. Hiraoka, and M. Yanagida.** 1984. Identification of the pleiotropic cell division cycle gene *NDA2* as one of two different alpha-tubulin genes in *Schizosaccharomyces pombe*. *Cell* **37**:233–242.
 53. **Tsai, W. Y., Y. T. Chow, H. R. Chen, K. T. Huang, R. I. Hong, S. P. Jan, N. Y. Kuo, T. Y. Tsao, C. H. Chen, and S. C. Cheng.** 1999. Cef1p is a component of the Prp19p-associated complex and essential for pre-mRNA splicing. *J. Biol. Chem.* **274**:9455–9462.
 54. **Urushiyama, S., T. Tani, and Y. Ohshima.** 1996. Isolation of novel pre-mRNA splicing mutants of *Schizosaccharomyces pombe*. *Mol. Gen. Genet.* **253**:118–127.
 55. **Vainberg, I. E., S. A. Lewis, H. Rommelaere, C. Ampe, J. Vandekerckhove, H. L. Klein, and N. J. Cowan.** 1998. Prefoldin, a chaperone that delivers unfolded proteins to cytosolic chaperonin. *Cell* **93**:863–873.
 56. **Vaisman, N., A. Tsouladze, K. Robzyk, S. Ben-Yehuda, M. Kupiec, and Y. Kassir.** 1995. The role of *Saccharomyces cerevisiae* *Cdc40p* in DNA replication and mitotic spindle formation and/or maintenance. *Mol. Gen. Genet.* **247**:123–136.
 57. **Vijayraghavan, U., M. Company, and J. Abelson.** 1989. Isolation and characterization of pre-mRNA splicing mutants of *Saccharomyces cerevisiae*. *Genes Dev.* **3**:1206–1216.
 58. **Wagner, J. D., E. Jankowsky, M. Company, A. M. Pyle, and J. N. Abelson.** 1998. The DEAH-box protein PRP22 is an ATPase that mediates ATP-dependent mRNA release from the spliceosome and unwinds RNA duplexes. *EMBO J.* **17**:2926–2937.
 59. **Weinstein, B., and F. Solomon.** 1990. Phenotypic consequences of tubulin overproduction in *Saccharomyces cerevisiae*: differences between alpha-tubulin and beta-tubulin. *Mol. Cell. Biol.* **10**:5295–5304.
 60. **Woods, A., T. Sherwin, R. Sasse, T. H. MacRae, A. J. Baines, and K. Gull.** 1989. Definition of individual components within the cytoskeleton of *Trypanosoma brucei* by a library of monoclonal antibodies. *J. Cell Sci.* **93**:491–500.
 61. **Yeong, F. M., H. H. Lim, C. G. Padmashree, and U. Surana.** 2000. Exit from mitosis in budding yeast: biphasic inactivation of the *Cdc28-Clb2* mitotic kinase and the role of *Cdc20*. *Mol. Cell* **5**:501–511.
 62. **Zhang, M. Q., and T. G. Marr.** 1994. Fission yeast gene structure and recognition. *Nucleic Acids Res.* **22**:1750–1759.